Design and Performance Evaluation of Multilayer Packaging Films for Blister Packaging Applications

S. W. Hwang,[1] J. K. Shim,[2] S. B. Lee,[2] R. Auras[1]

[1]School of Packaging, Michigan State University, East Lansing, Michigan 48824-1223
[2]Korea Institute of Technology, Korea Packaging Center, Bucheon-si, Gyeonggi-do, South Korea

ABSTRACT: Five multilayer packaging film structures consisting of amorphous poly(ethylene terephthalate) (APET), low-density polyethylene (LDPE), polypropylene (PP), and acrylonitrile/methyl acrylate copolymer (Barex) films [i.e., APET/polyethylene (PE), APET/PP, APET/PE + UV inhibitor, APET/PP/PE, and APET/Barex/PP] for blister packaging applications were designed and produced. Blister containers with APET/PE and APET/Barex/PP structures were prepared, and their optical, mechanical, barrier (O_2, CO_2, and H_2O), physical, and product/package compatibility performance properties were evaluated. Package/product compatibility with simulants (soy sauce and sunscreen skin cream) at 37.8°C was evaluated for 3, 7, 14, and 28 days in the multilayer films and the blister containers. APET/Barex/PP film showed significantly better O_2 and CO_2 barrier performance than the other four film structures. The UV inhibitor had no significant effect on the barrier properties in the APET/PE film structure. All of the film structures showed high enough elastic storage modulus values to be applied to blister packaging in a broad range of temperatures between −45 and 80°C. The glass-transition temperature of APET, which was responsible for the elastic modulus of the multilayer structure, decreased after the samples were exposed to the skin cream. This decrease may have been due to the sorption of the skin cream's active ingredients, such as ethylhexyl methoxycinnamate. © 2010 Wiley Periodicals, Inc. J Appl Polym Sci 116: 2846–2856, 2010

Key words: compatibility; polyesters; polyethylene (PE)

INTRODUCTION

Blister packaging is one of the most widely used thermoformed packaging systems for foods, cosmetics, and pharmaceutical applications because it is relatively easy to produce, has a low cost, and is effective for material shipping. Various packaging film materials, such as cellophane, polyolefin, polyamide, vinyl polymers, and polyester, are commonly used for blister packaging. However, many products cannot be adequately packaged with any of these polymeric materials alone, so multilayer structures of two or more materials are required for protection and shelf-life extension. Multilayer films are created to overcome the optical, mechanical, and/or barrier property limitations of single-layer films. Commercially developed multilayer structures are available, including Nylopak and Saranex barrier films (Dow Chemical Co., Midland, MI) and coextruded cyclic olefin copolymer blister pack films (Amcor Flexibles, Mundelein, IL).

Amorphous poly(ethylene terephthalate) (APET) films and sheets are suitable for thermoforming packaging applications where a higher strength is not the limiting challenging factor, such as in blister containers, multilayer trays, cups, and other thermoformed containers.[1] Barex, an acrylonitrile/methyl acrylate copolymer grafted onto a nitrile rubber, has been increasingly used for new multilayer structures because it has excellent barrier properties. Barex is typically used for rigid containers, such as thermoformed blisters for meat and cheese packaging.[2] Polyolefins, such as low-density polyethylene (LDPE) and polypropylene (PP), are commonly used for heat-sealable layers in multilayer film structures.

In addition to mechanical, physical, and barrier requirements, multilayer film structures must meet compatibility requirements between the polymeric films and the product. Mass transport phenomena between packages and products are a constant concern in the design of food and nonfood contact packaging systems. Understanding interactions, such as sorption, diffusion, migration, and flavor scalping, in packaging materials is very important for the preservation of the product quality and the packaging integrity. Flavor scalping, the loss of volatile organic compounds from a food into a polymeric packaging material, continues to be the subject of considerable attention and research.[3]

Flavor scalping is mostly described as the sorption, diffusion, and desorption process of gases, vapor, or organic permeants into polymers, and it is mainly described and modeled as a function of different factors or parameters, such as polymer/organic molecule chemistry, crystallinity, molecular orientation, physical aging, and polymer thermal history. For example, Paik and Writer[4] demonstrated that PP films absorbed less D-limonene than LDPE films during storage. Fayoux et al.[5] found that the sorption of aromatic compounds, such as orange juice and D-limonene, by plastic packaging materials like PP could cause unbalanced flavor profiles in the final product. In a study of myrcene and D-limonene sorption by refillable poly(ethylene terephthalate) (PET) bottles, various PET strips, and polycarbonate strips, Nielsen[6] found that polycarbonate absorbed these flavors to a much larger extent than PET and that the PET bottles absorbed significantly more of these flavors when stored at 25°C than at 4°C. Toebe et al.[7] studied the permeation and sorption of onion/garlic flavored sour cream on high-impact polystyrene containers. They did not detect the permeation of flavor components of sour cream, such as dipropyl disulfide and dimethyl disulfide, but found significant sorption of these compounds within the high-impact polystyrene. Safa et al.[8] found that the sorption of amyl acetate to PP increased with increases in the concentration of the amyl aceta and the temperature; amyl acetate showed a plasticizing effect on PP, which resulted in a decreased elastic modulus.

Because crystalline regions are highly ordered compared to amorphous regions, the free volume is lower or nonexistent in these regions. The crystalline regions act as excluded phases for the sorption process and as impermeable barriers for diffusion and sorption mechanics. Furthermore, crystalline regions present a constraint on the polymer chains in the amorphous region. This chain restriction influences the sorption process in the amorphous phase by limiting the effective pathlength of diffusion and reducing the polymer chain mobility, which creates a higher activation energy for diffusion. For many polymer/gas or organic vapor systems, the solubility coefficients are directly proportional to the free volume fraction of the amorphous phase.[9]

The thermal and mechanical histories to which a semicrystalline polymer have been exposed through processing play an important role in the final physical, mechanical, and barrier properties of the polymer. Qin et al.[10] showed that benzaldehyde followed a Fickian sorption in PP resin at low vapor activities and found much higher benzaldehyde solubility in a PP extruded sheet and thermoformed containers than in the resin, which explained the loss of benzaldehyde in the two PP containers. Moreover, Kumar et al.[11] investigated the effect of the container configuration on the barrier properties and sensory perception of cherry drinks. They found that water-vapor, oxygen, and aroma barriers of two PP containers that were shaped differently but had the same surface area were statistically different. Also, they reported that a difference of residual benzaldehyde in the two PP containers during storage was detectable by a trained sensory panel. Recently, Mokwena et al.[12] investigated the influence of a microwave (MW) sterilization process on the oxygen transmission rate of two multilayer films composed of ethylene vinyl alcohol (EVOH; middle layer), PET, and LDPE during storage with conventional retorting for comparison. They found that the oxygen barrier of the two films deteriorated during hot-water retorting and MW processing, but MW processing resulted in less oxygen barrier deterioration than the conventional process and could be used to reduce hydration of the EVOH layer because of its shorter processing time.

In the case of multilayer film structures where several layers of polymers are used, only one of the layers is in direct contact with the product. Therefore, any species not thermodynamically in equilibrium between the contact layer and the product will tend to equilibrate its chemical potential value and produce the sorption of chemical compounds in the layer and further on in the multilayer structure.[3] Noriega et al.[13] developed a computational model for predicting the water, oxygen, and carbon dioxide permeability values of multilayer structures made from combinations of EVOH, PP, and polyethylene (PE) films to meet the requirements of a specific food and/or beverage systems. However, the design and final barrier properties to organic compounds for multilayer structures include many more scenarios.

In this study, five multilayer films were designed and evaluated to determine the most suitable structure to produce blister packages for selected food and cosmetic products. The multilayer structures were designed to achieve oxygen, carbon dioxide, and water barrier permeance values of 8.16×10^{-16}, 4.49×10^{-15}, and 5.71×10^{-13} kg m^{-2} Pa^{-1} s^{-1}, respectively, which prevented a maximum loss of 0.007 g of O_2, 0.04 g of CO_2, and 5 g of H_2O per square meter daily. These values are becoming target values for food and cosmetic packaging applications. In addition, the optical, barrier, thermal, physical, and mechanical properties of the multilayer films and containers were investigated in a compatibility study with two simulants, soy sauce and sunscreen skin cream. The sorption values of these two simulants by the multilayer films and containers were also evaluated.

<div align="center">

TABLE I
Material Characteristics of the Films Used To Form Multilayer Structures

</div>

Film	Melt flow index (g/10 min)	Density (g/cm^3)	Trade name (source)
APET	Not applicable	1.40	TB-380 (Honam Petrochemicals, Seoul, South Korea)
LDPE	2.0	0.922–0.926	BF 415 (LG Chemicals, Seoul, South Korea)
PP	12.0	0.900	DJ-550S (Honam Petrochemicals, Seoul, South Korea)
Barex	3.0	1.15	Barex (BP Chemicals, Lima, OH)

EXPERIMENTAL

Materials

APET and PP were provided by Honam Petrochemical Co., Ltd. (Seoul, South Korea). LDPE was obtained from LG Chemicals (Seoul, South Korea). Barex film was purchased from BP Chemicals (Lima, OH). The melt flow index and density characteristics provided by the manufacturers of the materials are given in Table I. The UV inhibitor was obtained from SKC Co., Ltd. (Suwon, South Korea). Urethane adhesive (Seongdo Chemical, Hwasung, South Korea) was used to laminate the films and was dissolved in mixed solvents (methyl acetate and methyl ethyl ketone with a 1 : 1 volume fraction).

Preparation of the multilayer film structures

To prepare the multilayer film structures, urethane adhesive was first applied to one surface of the APET film at room temperature. The two-layer films (APET/PE, APET/PE + UV, APET/PP, and APET/Barex) were laminated between rotating rollers of a dry laminator (Hanyoung Machinery Co., Seoul, South Korea). To remove the solvents in the adhesive, the laminated films were passed through an oven at 50°C for 15 min at a rolling speed of 80 m/min. The three-layer films (APET/PP/PE and APET/Barex/PP) were prepared by the lamination of a third layer to the two-layer APET/PP and APET/Barex structures; urethane adhesive was applied to the surface of the PP layer or film, and lamination was carried out as described previously. Adhesive solvents were removed under the same oven conditions mentioned previously. Finally, the three-layer films were aged at 50°C for 24 h to enhance the adhesion strength between films. The characteristics of the produced multilayer films are given in Table II.

Preparation of the blister containers

Blister containers were prepared from the APET/PE and APET/Barex/PP multilayer films with an automatic blister packaging machine (Blispack Co., Ansan, South Korea). The multilayer films were pressed in the blister molds at 170°C for 1 s and then allowed to cool to room temperature.

Optical and structural properties of the films

The total color difference (ΔE^*) of the multilayer films after immersion in the simulants was measured with a ColorQuest colorimetric spectrometer (Hunter Associates Laboratory, Reston, VA). The transmitted color was presented with the Commission Internationale de l'Eclairage $L^*a^*b^*$ color scale.

Thermomechanical properties of the films

Dynamic mechanical analysis (DMA) of the multilayer film structures was performed on a DMA Q800 instrument (TA Instruments, New Castle, DE) in accordance with ASTM D 4065. Film samples 5.8–6.5 mm in width and 25–30 mm in length were cut for DMA testing in the tension mode. The sample dimensions were carefully measured, and the mean values of six measurement points of the samples were entered into the program that controlled the instrument. The measurement was carried out at a heating rate of 5°C/min over a temperature range of −65 to 100°C and at a frequency of 1 Hz. The storage modulus (G'), loss modulus (G''), and loss tangent (tan δ) were studied for each sample in this temperature range. The glass-transition temperature (T_g) was determined at the maximum G'' because the maximum energy loss occurred at T_g. The data were analyzed with Universal Analysis 2000 software (TA Instruments).

Oxygen, carbon dioxide, and water-vapor barrier properties of the films

Gas-transmission rates (GTRs) of oxygen (O_2), carbon dioxide (CO_2), and water vapor (H_2O) of the

<div align="center">

TABLE II
Characteristics of the Multilayer Films

</div>

Sample	UV inhibitor	Transparency	Thickness (mm)
APET/PE	No	Yes	0.218 ± 0.003
APET/PP/PE	No	Yes	0.385 ± 0.004
APET/PE + UV	Yes	No	0.296 ± 0.002
APET/PP	No	Yes	0.401 ± 0.001
APET/Barex/PP	No	Yes	0.426 ± 0.006

All of the values are expressed as average values and standard deviations.

multilayer film structures were measured with an Illinois 8001 system (O_2; Illinois Instruments, Inc., Johnsburg, IL), a Permatran C 4/41 (CO_2), and a Permatran W 3/33 (H_2O; Modern Controls, Inc., Minneapolis, MN). The tests were performed in accordance with ASTM 3985 and ASTM 1927 (O_2), ASTM F2476 (CO_2), and ASTM F1249 (H_2O). For the O_2 test, film samples were placed in a diffusion chamber. Pure O_2 was then introduced into the upper half of the chamber while an oxygen-free N_2 carrier gas flowed through the lower half. O_2 molecules diffusing through the film into the lower chamber flowed to the sensor by the carrier gas measuring the GTR value. The GTRs for CO_2 and H_2O were also determined by the same technique. The temperature and relative humidity conditions were 23°C and 0% RH for the O_2 and CO_2 tests and 37.8°C and 100% RH for the H_2O test. The O_2 and CO_2 gases (Airgas, Inc., Lansing, MI) at 99.99% concentrations and high-performance liquid chromatography (HPLC) grade water (Sigma–Aldrich, St. Louis, MO) were used as permeants. The GTR was calculated by the averaging of the last 10 constant values for duplicate samples. The permeance of O_2 and CO_2 were calculated with eq. (1), and the permeability of H_2O was obtained with eq. (2):

$$\text{Permeance (Film)} = \text{Gas Transmission Rate}$$
$$\times \frac{1}{\Delta P}\left(\frac{\text{kg}}{\text{m}^2 \cdot \text{Pa} \cdot \text{s}}\right) \quad (1)$$

$$\text{Permeance (Film)} = \text{Water Vapor Transmission Rate}$$
$$\times \frac{1}{\Delta P}\left(\frac{\text{kg}}{\text{m}^2 \cdot \text{Pa} \cdot \text{s}}\right) \quad (2)$$

where ΔP is the difference in the permeant partial pressure across the films in the Pascal (Pa).

O_2 and H_2O vapor barrier properties of the blister containers

The O_2 and H_2O transmission rates for the blister containers were determined with the same techniques previously described for the films. The simulant (soy sauce or skin cream) filling the inside of the blister container was emptied and carefully wiped out after the compatibility test, and the container was sealed onto a metal plate designed for package testing. The plate plus the containers were connected to the Illinois 8001 system with copper tubing that carried nitrogen in and out of the blister containers. The test was performed with air as the permeant gas, and the results were compensated to 100% oxygen at 23°C. For water vapor transmission rate (WVTR), the same plate was used to mount the

blister containers, and it was connected to the Permatran W 3/33 system. The system was covered with a PE pouch, and wet sponges were used inside of the pouch to produce 100% RH conditions at 37.8°C. The permeability was calculated with eqs. (1) and (2), but the film area was replaced by the package.

Compatibility test for the multilayer films

The compatibility between the multilayer film structures and the two test simulants was determined. The simulants (1) Kikkoman soy sauce (Kikkoman Foods, Inc., Walworth, WI) and (2) Natria sunscreen skin cream (Nature's Sunshine Products, Inc., Spanish Fork, UT) were chosen for the test as model products for food and cosmetic packaging. The film samples (6.5 × 45 mm^2) were immersed in 20-mL vials filled with simulant 1 or 2, and both sides of the sample were in contact with the simulant. The immersed samples were stored at 37.8°C (i.e., accelerated conditions) in a Peltier effect temperature cabinet (Sable Systems International, Las Vegas, NV) for 3, 7, 14, and 28 days. The samples were carefully wiped off after each storage period, and then, the weight change and dimension change were measured. The optical and thermomechanical properties were characterized by DMA as described later. Four samples of each film were used for the tests.

Compatibility test for the blister containers

The blister containers were filled with the simulants (soy sauce or skin cream) inside a glove box (Labconco Corp., Kansas City, MO) to avoid contamination during the filling process. The glove box was sterilized with a 2% chloride solution (The Clorox Co., Oakland, CA) before it was filled, and a nitrogen positive pressure was maintained during filling. After containers were filled, an aluminum lid film (Lotte Aluminum Co., Ltd., Seoul, South Korea) was heat-sealed onto the blister tray with a custom-made blister packaging heat sealer at 210°C for 1.5 s. A schematic of the blister-sealing process is shown in Figure 1. A seal integrity test was performed with a vacuum method in accordance with ASTM D 4991. The same procedure used for the multilayer films
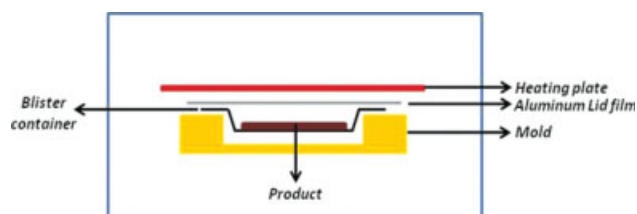

Figure 1 Schematic of the blister-sealing process. [Color figure can be viewed in the online issue, which is available at www.interscience.wiley.com.]

was carried out to determine the compatibility between the formed blisters and the model products. The inside layer (PE and PP layer) of the APET/PE and the APET/Barex/PP blisters, respectively, were in contact with the simulants. The blisters were filled with either soy sauce or skin cream and stored at 37.8°C in a Peltier effect temperature cabinet for 3, 7, 14, and 28 days. The compression strength and weight changes of the blister packs were recorded after each period, and then, the products were carefully emptied and wiped out for further barrier property evaluation. The crush resistance of the blister pack was measured with a compression tester from Lansmont Corp. (Lansing, MI) in accordance with ASTM D 695. The preload was 0, the yield was 50%, and the stop force was 1000 lbs. Five samples were measured for each type of blister container.

Sorption study of the films

The separation of the absorbed component from the skin cream into the multilayer films after immersion was performed with a Micromass Q-Tof API (where Q-Tof is quadrupole time of flight and API is mass spectrometer with the atmosphere pressure ionization) with a Waters 2795 high-performance liquid chromatograph (LC–MS; Waters Corp., Milford, MA). A Thermo BETASIL Phenyl/Hexyl Column (inside diameter = 150 × 2.1 mm, 5 μm; Thermo Fisher Scientific, Inc., Waltham, MA) was used with a flow rate of 0.5 mL/min and a column temperature of 40°C. Methanol and dichloromethane (CH_2Cl_2; Sigma–Aldrich) were used as the mobile phase. The mobile phase for the initial 1 min and final 2 min was set with 100% methanol, and the composition of the mobile phase was programmed to be changed during the run: 25 : 75 at 10 min and 5 : 95 at 18 min.

We extracted chemical compounds from the control and submerged films by submitting the film samples to ultrasound (ultrasonic cleaner, Cole–Palmer, Vernon Hills, IL). The controls were prepared from the original films with no immersion in the simulants. Each film sample was weighed and transferred to a 20-mL vial, and 10 mL of 100% pure isopropyl alcohol (Mallinckrodt Baker, Inc. Phillipsburg, NJ) was added. The samples were sonicated for 10 min at room temperature; 10μL of extracted solution was then transferred to an HPLC vial for LC–MS analysis. A standard calibration for the quantitative analysis was prepared by the dissolution of one active ingredient of the skin cream formula, an ethylhexyl methoxycinnamate (EHMC; Sigma–Aldrich) in isopropyl alcohol. The final concentrations were 250, 500, 750, and 1000 ppm (μg/mL; $R^2 = 0.950$).
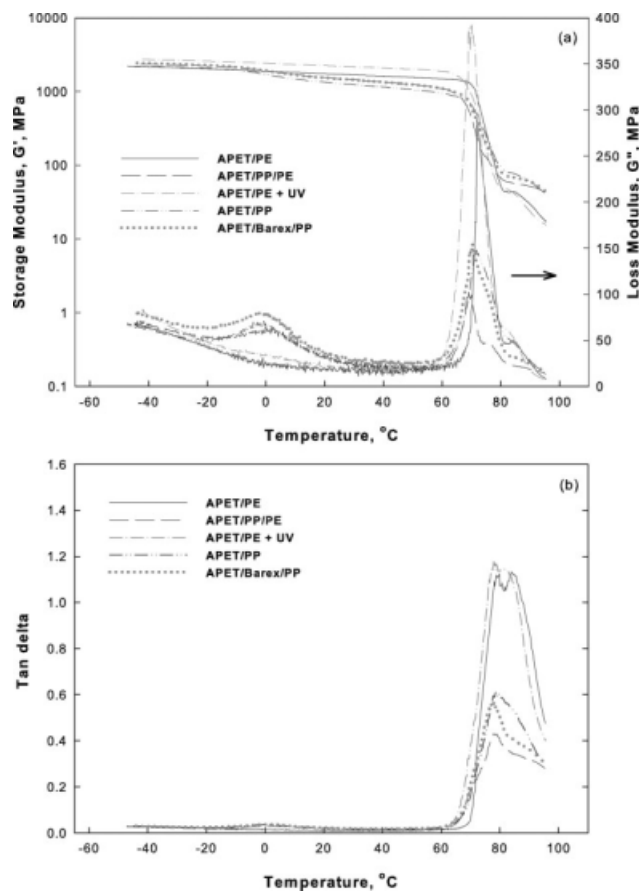

Figure 2 (a) G' and G'' and (b) tan δ peaks of the multilayer films.

Statistical analysis

Statistical analyses of the film properties data were performed with SPSS software (SPSS, Inc., Chicago, IL). One-way analysis of variance and Tukey' s honestly significant difference tests were used to determine significant differences [α (significant level) = 0.05].

RESULTS AND DISCUSSION

Initial characterization of the multilayer films

Thermomechanical properties

The results of temperature versus G' and G'' for all of the films at time zero from the DMA test are shown in Figure 2. Blister packages are thermally formed by a thermoforming process to various shapes in a range of temperatures. To make this process possible, polymeric films must have enough elasticity to hold their shape during the process. G' is a response of the elastic nature of the polymers. In this study, APET was incorporated to provide the storage modulus of the multilayer film structure. So, all of the multilayer film structures showed enough elastic modulus for thermoforming in a broad range

TABLE III
Permeability of the Multilayer Film Structures

Sample [thickness (mm)]	O_2 permeance ($\times 10^{-15}$ kg/m^2 Pa s)	CO_2 permeance ($\times 10^{-14}$ kg/m^2 Pa s)	Water vapor permeance ($\times 10^{-12}$ kg/m^2 Pa s)
APET/PE (0.218 ± 0.003)	3.51 ± 0.01[a]	1.68 ± 0.01[a]	1.70 ± 0.02[a]
APET/PP/PE (0.385 ± 0.004)	2.73 ± 0.00[b]	1.36 ± 0.00[b]	0.63 ± 0.00[b]
APET/PE + UV (0.296 ± 0.002)	2.68 ± 0.00[c]	1.45 ± 0.00[c]	1.28 ± 0.00[c]
APET/PP (0.401 ± 0.001)	2.43 ± 0.06[d]	1.36 ± 0.00[b]	2.40 ± 0.03[d]
APET/Barex/PP (0.426 ± 0.006)	0.89 ± 0.01[e]	0.087 ± 0.00[d]	2.34 ± 0.10[e]

Values in the same column with different superscript letters were significantly different at $\alpha = 0.05$; all of the values are expressed as average values and standard deviations.

of temperatures from −45 to approximately 80°C. Three films containing PP (APET/PP/PE, APET/PP, and APET/Barex/PP) showed a slight decrease in G' after 0°C because of the glass-transition region of PP. The tan δ values of the films with PP were also lower than those of the other films, which was attributed to the higher elastic modulus of PP than of PE, and resulted in a lower G'' of the film structure.

Barrier properties

The results of the gas permeance of the films are presented in Table III. Because the laminated multilayer film structures had different thicknesses, the permeance values were compared. All of the film structures showed different O_2 gas permeance values. APET/PP/PE, APET/PE + UV, and APET/PP had lower O_2 and CO_2 permeance than APET/PE because of their higher thicknesses. APET/Barex/PP had higher O_2 and CO_2 barrier properties than the

other four multilayer films because of the higher gas barrier properties of Barex, although the presence of Barex had almost no effect on the water-vapor permeance. As expected, the introduction of a PP layer into the APET/PE film structure significantly decreased the water-vapor permeance because of its high barrier properties. In addition, the UV inhibitor had no significant effect on the barrier properties of the APET/PE film structure when the thickness was normalized.

Compatibility test for the multilayer films

Optical and structural properties

ΔE^* values for the multilayer film structures immersed in the soy sauce and skin cream simulants are shown in Table IV. After the samples were exposed to soy sauce, the APET/PE and APET/PP/PE film structures showed significant changes in

TABLE IV
ΔE^* of the Films After Immersion in Soy Sauce or Skin Cream

Simulant	Immersion time (days)	ΔE^*			
		APET/PE	APET/PP/PE	APET/PP	APET/Barex/PP
Soy sauce	3	1.41 ± 0.21[a]	1.01 ± 0.17[a]	1.35 ± 0.08[a]	1.52 ± 0.68[a]
	7	2.35 ± 0.08[b]	2.87 ± 1.19[b]	1.48 ± 0.66[a]	1.34 ± 0.06[a]
	14	2.07 ± 0.29[b]	2.02 ± 0.10[b]	1.49 ± 0.32[a]	1.64 ± 0.43[a]
	28	2.16 ± 0.44[b]	2.16 ± 0.20[b]	1.34 ± 0.11[a]	1.15 ± 0.13[a]
Skin cream	3	0.84 ± 0.62[a]	0.53 ± 0.07[a]	0.52 ± 0.31[a]	1.25 ± 0.66[a]
	7	0.92 ± 0.15[a]	0.41 ± 0.05[a]	1.13 ± 0.25[ab]	1.14 ± 0.18[a]
	14	0.81 ± 0.28[a]	0.50 ± 0.07[a]	0.98 ± 0.49[bc]	1.18 ± 0.16[a]
	28	1.15 ± 0.17[a]	0.80 ± 0.14[b]	1.51 ± 0.18[c]	1.10 ± 0.11[a]

Values in the same column with different superscript letters were significantly different at $\alpha = 0.05$; all of the values are expressed as average values and standard deviations:

$$\Delta E^* = \sqrt{(\Delta L^*)^2 + (\Delta a^*)^2 + (\Delta b^*)^2}$$

$$\Delta L^* = L^*_{sample} - L^*_{standard}$$

$$\Delta a^* = a^*_{sample} - a^*_{standard}$$

$$\Delta b^* = b^*_{sample} - b^*_{standard}$$

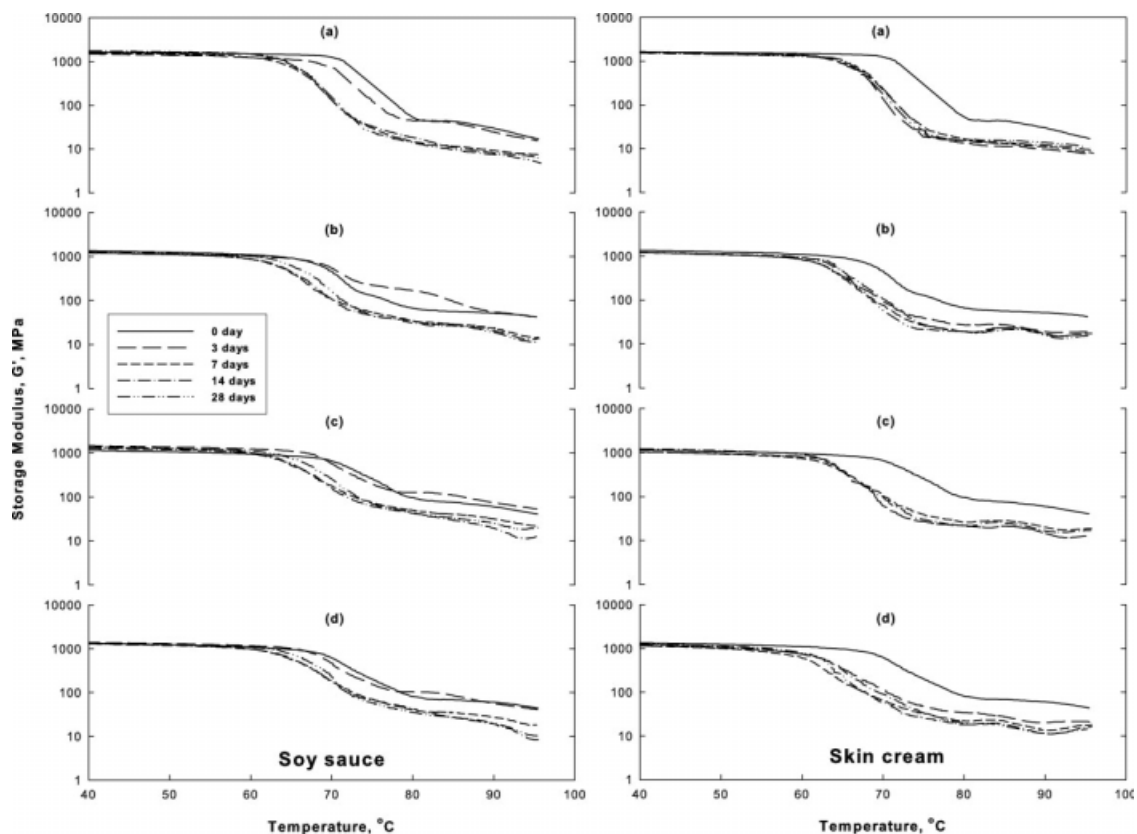The standard value was the initial value of the film before the sample was immersed.

Figure 3 Effect of the compatibility test for soy sauce and skin cream on G' of the multilayer films: (a) APET/PE, (b) APET/PP/PE, (c) APET/PP, and (d) APET/Barex/PP.

color from the standard value obtained from the original (unexposed) film structures, whereas APET/PP and APET/Barex/PP showed no differences. The L^* and a^* values did not change over the storage time for any of the film structures (data not shown). Therefore, the significant color changes were attributed to higher b^* values and were likely due to the sorption of chemical compounds that caused the samples to appear more yellow. After exposure to the skin cream, APET/PE and APET/Barex/PP showed

no significant color changes. APET/PP/PE and APET/PP did show statistically significant differences in ΔE^* value over time; however, these changes were not perceived with the naked eye.

Thermomechanical properties

Figure 3 shows the effects of the compatibility test on the G' changes over the immersion time. After 28 days, any sorption of compounds from the simulants

TABLE V
T_g **Changes in the Multilayer Films After Immersion in Soy Sauce or Skin Cream**

Simulant	Immersion time (days)	T_g (°C)			
		APET/PE	APET/PP/PE	APET/PP	APET/Barex/PP
Soy sauce	0	70.4 ± 1.4^a	68.8 ± 0.4^a	70.3 ± 1.3^a	69.7 ± 0.9^a
	3	69.6 ± 1.8^a	67.8 ± 1.8^a	70.0 ± 5.6^a	70.0 ± 5.2^a
	7	66.6 ± 0.6^b	63.3 ± 0.6^b	64.2 ± 0.3^b	64.4 ± 0.8^b
	14	67.3 ± 1.0^b	64.6 ± 0.9^{bc}	65.7 ± 1.1^{ab}	65.2 ± 0.3^{ab}
	28	65.9 ± 0.4^b	65.6 ± 0.4^c	65.8 ± 1.0^{ab}	66.2 ± 0.3^{ab}
Skin cream	0	70.4 ± 1.4^a	68.8 ± 0.4^a	70.3 ± 1.3^a	69.7 ± 0.9^a
	3	66.8 ± 1.8^b	63.7 ± 0.2^b	66.8 ± 1.8^b	63.2 ± 0.5^b
	7	67.2 ± 0.7^b	63.7 ± 0.8^b	64.0 ± 0.6^b	62.9 ± 1.1^b
	14	67.3 ± 0.6^b	64.5 ± 0.6^b	64.6 ± 1.2^b	64.5 ± 0.4^b
	28	66.6 ± 0.0^b	64.5 ± 0.0^b	64.3 ± 0.2^b	63.2 ± 0.9^b

Values in the same column with different superscript letters were significantly different at $\alpha = 0.05$; all of the values are expressed as average values and standard deviations.
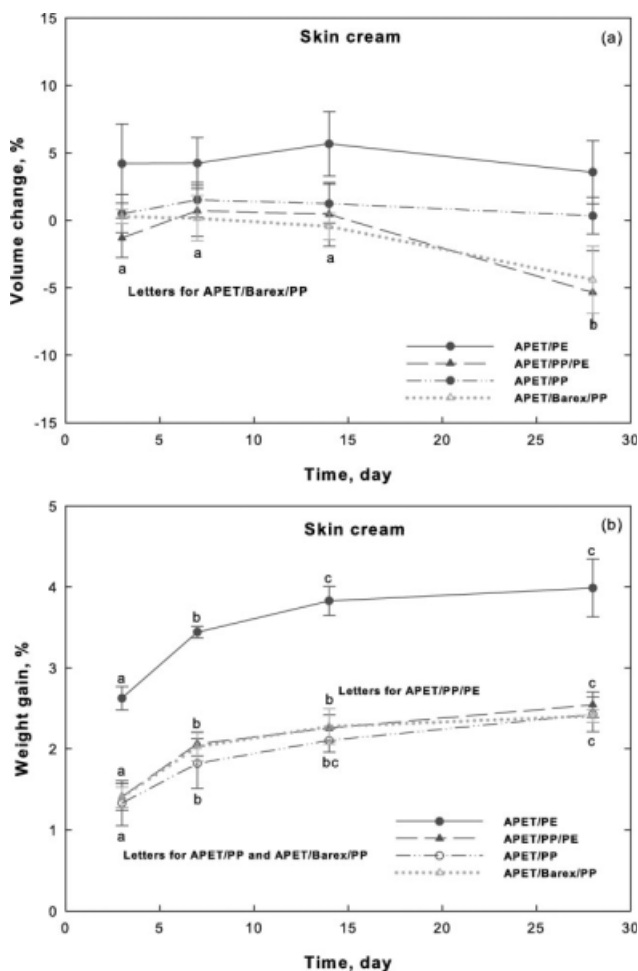
Figure 4 (a) Volume change and (b) weight gain of the film structures after immersion in skin cream. For each multilayer film over time, values with different letters were significantly different at $\alpha = 0.05$.

by the films appeared to have little effect on G'. However, T_g of the APET layer of the multilayer films exposed to the simulants significantly decreased after 7 days (soy sauce) and 3 days (skin cream), respectively, as shown in Table V. We assumed that the sorption of compounds from the simulants by the films produced a plasticizing effect on the amorphous region of PET and resulted in a decreased T_g.

Dimensional stability

No statistically significant changes in volume or weight were detected in any of the films immersed in soy sauce for up to 28 days; this indicated good dimensional stability (data not shown). Immersion in the skin cream resulted in statistically significant differences in the volume change only for APET/Barex/PP after 28 days [Fig. 4(a)]. A significant difference in weight gain was found for all of the film structures. However, the dimensional stability of the films was maintained throughout the test [Fig. 4(b)].

Sorption study

LC–MS chromatograms of the APET/PP/PE film structure before (control) and after immersion in skin cream are presented in Figure 5. Chromatograms obtained for all other multilayer films were similar (not shown). The sunscreen skin cream was composed of many organic compounds. Among them, EHMC was found at 1.30 min of retention time for the samples submerged in the skin cream but not in the control. EHMC is an active ingredient widely used in sunscreen creams for the UV protection of skin. Figure 6 shows the EHMC
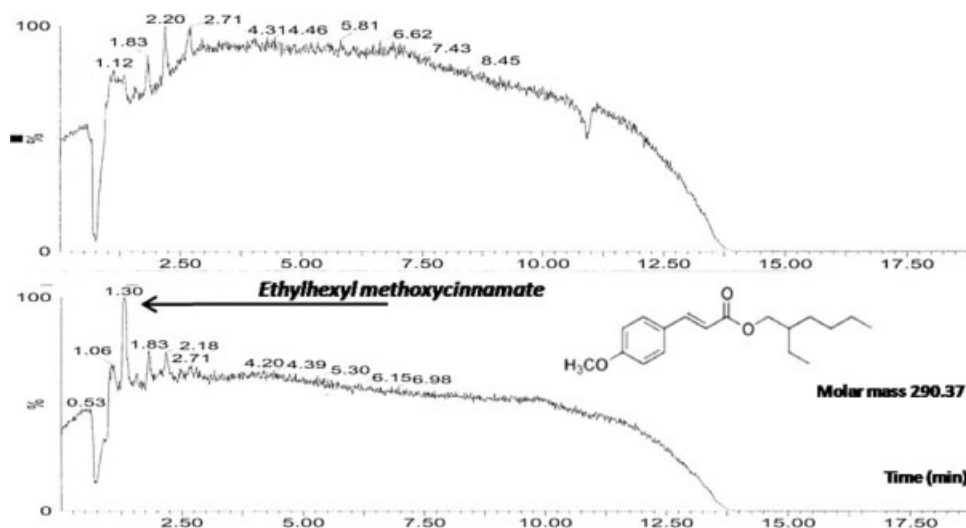

Figure 5 LC–MS chromatograms of the extract from the APET/PP/PE film (the control is shown on the top, and the sample after 3 days of immersion in skin cream is shown on the bottom).
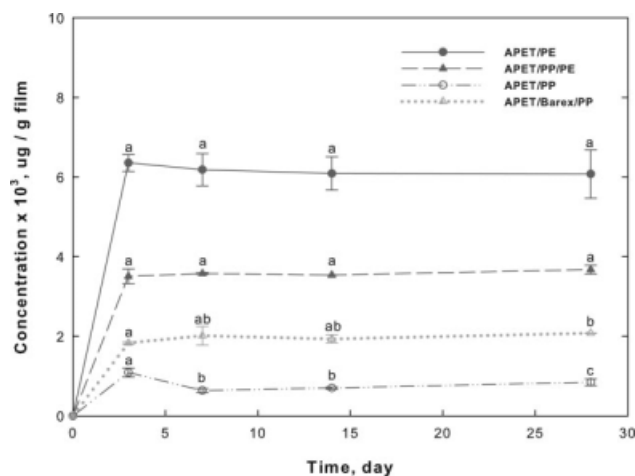
Figure 6 Concentration of EHMC with respect to the immersion time for all of the multilayer films. For each multilayer film over time, values with different letters were significantly different at α = 0.05.

concentrations (μg/mL) in the films as a function of the immersion time. The film structures with PE showed high concentrations of EHMC, likely because of the similarity between their solubility parameters. The solubility parameters for APET, PE, and EHMC were calculated by the average of the Hoftyzer–Van Krevelen and the Hoy group contribution methods.[14–16] The estimated solubility parameters [i.e., dispersion bonding (δ_d), polar (δ_p), hydrogen (δ_h)] were found to be 16.85 (δ_d), 11.82 (δ_p), 11.94 (δ_h), and 24.70 (δ_T) for PET; 17.92 (δ_d), 0 (δ_p), 0 (δ_h), and 17.92 (δ_T) for PE; 16.60 (δ_d), 0 (δ_p), 0 (δ_h), and 16.60 (δ_T) for PP, and 15.32 (δ_d), 5.888 (δ_p), 8.528 (δ_h), and 18.99 (δ_T) for EHMC. Three films had a similar dispersion bonding solubility parameter, but the total solubility parameter of PE was closest to that of EHMC; this suggested that LDPE may have absorbed more EHMC.

Compatibility test for the blister containers

Mechanical properties: Compression strength

Figure 7 shows the maximum force necessary to compress the blister containers filled with soy sauce or skin cream as a function of immersion time. Both the APET/PE and APET/Barex/PP blisters showed some significant differences in the compression strength after immersion in the simulants. According to ASTM D 4991, the compression results of the sealed containers depended on the seal strength between the lid films and containers. Although the integrity test of the blister containers confirmed the complete seal of the container, there might have been defects between the lid film and container that caused variation in the results. The APET/Barex/PP container had a lower average maximum force than

the APET/PE container because of an easy peel treatment on the top PP layer. In addition, the average maximum force for the APET/PE container tested with skin cream showed lower values than that for the container tested with soy sauce. This difference may have been due to the filling process, which required a much larger headspace in the soy sauce containers to prevent the soy sauce from spilling out during sealing. Therefore, there was a different internal pressure in the soy sauce and skin cream in the containers; this resulted in different final compression strengths. However, no difference in the compression strength was found in the APET/Barex/PP container in either simulant. The easy peel treatment of the PP layer made no difference in the compression strength, regardless of internal pressure.

Barrier properties

The results of the O_2 and H_2O permeability tests of the containers as a function of immersion time are
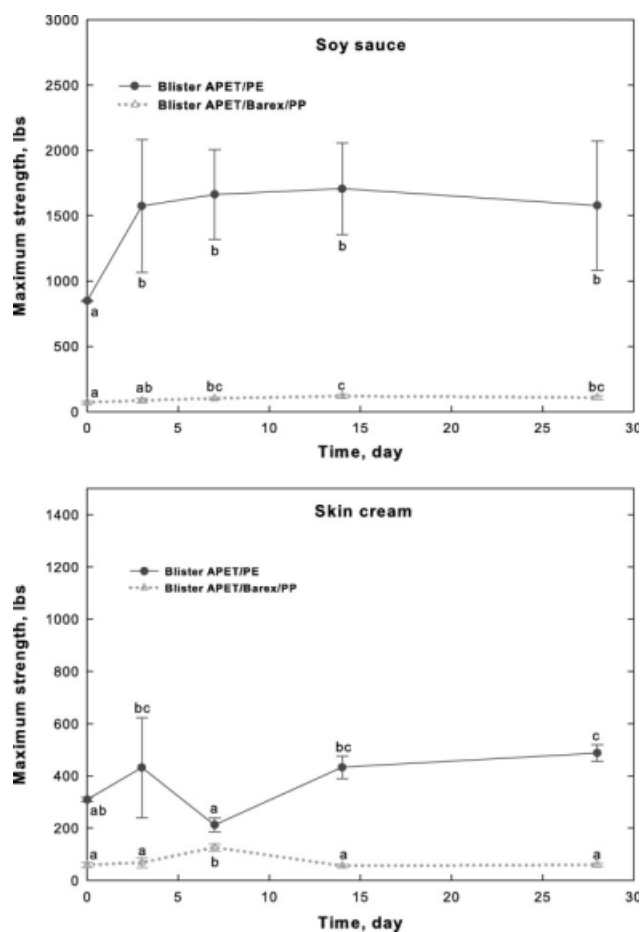

Figure 7 Compression strength of the blister packs after immersion in soy sauce or skin cream. For each multilayer blister over time, values with different letters were significantly different at α = 0.05.

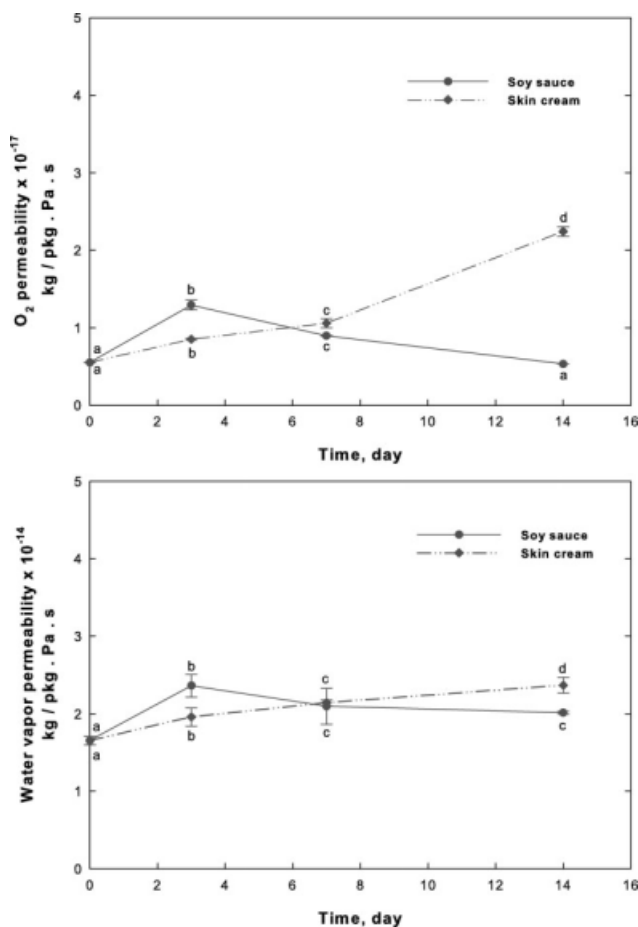**Figure 8** O_2 and H_2O permeability of the APET/PE blister pack with respect to immersion in simulants over time. For each simulant over time, values with different letters were significantly different at $\alpha = 0.05$.

presented in Figures 8 and 9. The O_2 and H_2O permeability of the blisters made of APET/PE tested with skin cream increased as time went on (Fig. 8). This decrease in the barrier properties may have been due to the sorption of EHMC, which may have increased the free volume between the polymer chains and resulted in an increase in the permeability. In the case of APET/Barex/PP, the sorption of EHMC was much lower, as indicated in Figure 6. Although a statistical difference was observed, the changes were small, so they should not have had a large effect on the barrier properties.

Weight change

The weight loss values of the multilayer blister containers during immersion in simulants in the compatibility test are shown in Figure 10. The APET/PE container lost 1.8 ± 0.1 and 1.7 ± 0.1 wt % after 28 days in the soy sauce and skin cream, respectively. The APET/Barex/PP container lost 1.2 ± 0.2 and 1.3 ± 0.2 wt % after 28 days in the respective simulants. Both containers showed the same weight loss

regardless of the simulants. More weight loss was expected for the APET/Barex/PP container because of the higher H_2O permeability than the APET/PE container. We inferred that the H_2O permeability was not the only factor affecting the weight loss (see Table III). However, for both multilayer structures, these low weight loss values would be acceptable for blister packages for food and cosmetic applications.

CONCLUSIONS

Five different multilayer film structures were produced, and their optical, physical, thermomechanical, and barrier properties were evaluated. Two of these structures, APET/PE and APET/Barex/PP, were used to produce blister containers. The compatibility of the multilayer films and blister containers with two simulants was assessed. As expected, the presence of Barex film greatly enhanced the O_2 and CO_2 barrier properties of the multilayer structures but had no effect on the H_2O barrier properties. The target values for the O_2 and CO_2 barrier
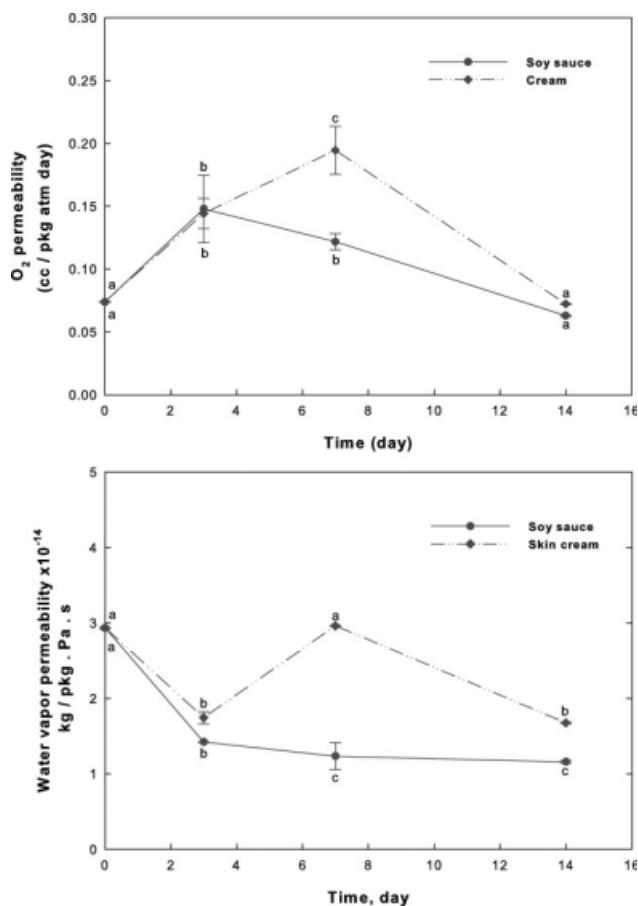

Figure 9 O_2 and H_2O permeability of the APET/Barex/PP blister pack with respect to immersion in simulants over time. For each simulant over time, values with different letters were significantly different at $\alpha = 0.05$.
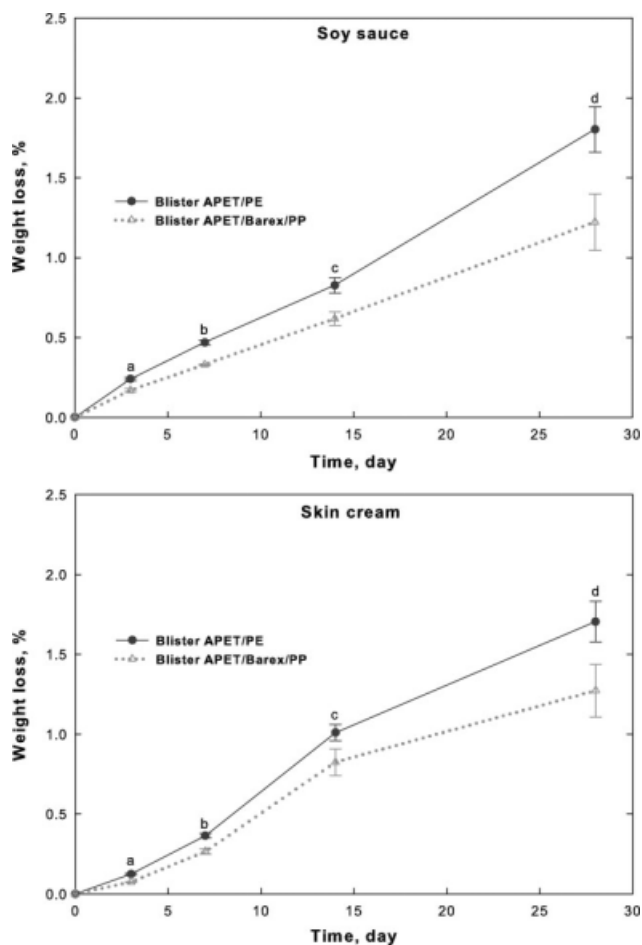
Figure 10 Weight loss of the blister packs after immersion in soy sauce or skin cream. For each multilayer blister over time, values with different letters were significantly different at α = 0.05.

properties were achieved, but those of the H$_2$O barriers were not. This suggests that a thicker PP layer would be required. The presence of the UV inhibitor had no significant effect on the barrier properties of the APET/PE structure when the permeability values were normalized by a consideration of the film thickness. Also, the APET film was responsible for the elastic modulus of the whole film structure. T_g of the APET film decreased significantly after immersion in the skin cream and soy sauce for 3 and 7 days, respectively. It was demonstrated that

that the sorption of EHMC from the skin cream into the multilayer films reduced the T_g of APET. In the compatibility test, all of the film structures showed no volume or weight change after immersion in the soy sauce. No major compatibility performance issues were observed between these products and the containers. However, because of the sorption of EHMC, a sunscreen active ingredient, into the APET film, a reduction in the shelf life of the skin cream could be expected.

References

1. Forman, C.; Zinoviev, P. A. High-Performance Films; CRC: Boca Raton, FL, 1996.
2. Selke, S.; Culter, J. D.; Hernandez, R. J. Plastics Packaging: Properties, Processing, Applications, and Regulations, 2nd ed; Hanser Gardner: Cincinnati, OH, 2004.
3. Hernandez, R. J.; Giacin, J. R. In Food Storage Stability; Taub, I. A.; Singh, R. P., Eds.; CRC: Boca Raton, FL, 1998; Chapter 10.
4. Paik, J. S.; Writer, M. S. J Agric Food Chem 1995, 43, 175.
5. Fayoux, S. C.; Seuvre, A.; Voilley, A. J. Packag Technol Sci 1997, 10, 145.
6. Nielsen, T. J. J Food Sci 1994, 59, 227.
7. Toebe, J.; Hoojjat, H.; Hernandez, R. J.; Giacin, J.; Harte, B. Packag Technol Sci 1990, 3, 133.
8. Safa, L.; Abbes, B.; Zaki, O. Packag Technol Sci 2007, 20, 403.
9. Sanders, E.; Koros, W.; Hopfenberg, H.; Stannett, V. J Membr Sci 1984, 18, 53.
10. Qin, Y.; Rubino, M.; Auras, R.; Lim, L. T. Polym Test 2007, 26, 1082.
11. Kumar, P.; Auras, R.; Rubino, M.; Almener, E.; Harte J. Presented at the 23rd International Association of Packaging Research Institutes; Symposium on Packaging, Windsor, UK, September 3–5, 2007.
12. Mokwena, K. K.; Tang, J.; Dunne, C. P.; Yang, T.; Chow E. J Food Eng 2009, 92, 291.
13. Noriega, M. P.; Estrada, O.; Vargas, C. A. In Proceedings of the Annual Technical Conference, Nashville, TN; The Society of Plastics Engineers, Brookfield, Connecticut, 2003; p 3218.
14. VanKrevelen, D. W. Properties of Polymers, 3rd ed.; Elsevier Science: Amsterdam, The Netherlands, 1997.
15. Hansen, C. M. Hansen Solubility Parameters: A User's Handbook; CRC: Boca Raton, FL, 2007.
16. Barton, A. F. M. CRC Handbook of Solubility Parameters and Other Cohesion Parameters; CRC: Boca Raton, FL, 1991.